The Abdus Salam International Centre for Theoretical Physics

United Nations Educational, Scientific and Cultural Organization

IAEA International Atomic Energy Agency

Conference on Time Crystals | (SMR 3593)

08 Mar 2021 - 10 Mar 2021
Virtual, Virtual, Italy

P01 - COSME Gutierrez Jayson

Controlling phases and time crystal in an atom-cavity system

P02 - DOS PRAZERES Fernando Luis

Boundary time crystals in collectived-level systems

P03 - FAN Chuhui

Realization of time-space lattices

P04 - GIERGIEL Krzysztof

Anderson Molecules: Bound States of Atoms due to Anderson Localization

P05 - GOLLETZ Weronika

Phase diagram and optimal control for n-tupling discrete time crystal

P06 - KELLY Shane Patrick

Stroboscopic aliasing in long-range interacting quantum systems

P07 - KONGKHAMBUT Phatthamon

Dissipative Time Crystals in an atom-cavity system

P08 - KUROŚ Arkadiusz

Non-separable time-crystal structures on the M\

P09 - ODEYEMI Olusanmi Ebenezer

Structural, Electronic, Magnetic and Thermodynamic Properties of XCrGe (X = Hf and Zr) Half-Heusler compounds: First Principle Calculations

P10 - SCARLATELLA Orazio

Dynamical Mean-Field Theory for Markovian Open Quantum Many-Body Systems

P11 - SHAH Muhammad Ali Zaheer Syed

Towards a Time Crystal Based on a Bouncing Bose-Einstein Condensate

P12 - SKULTE Peter Jim

Incommensurate time crystalline dynamics in a atom-cavity system

P13 - SMITS Jasper

On the long-term stability of space-time crystals

P14 - SUTHAR Kuldeep

Many-body localization with synthetic gauge fields in disordered Hubbard chains

P15 - TYLUTKI Jan Marek

Universal Aspects of Vortex Reconnections across the BCS-BEC Crossover

P01

Controlling phases and time crystal in an atom-cavity system

Periodic driving of strongly correlated systems has led to outstanding discoveries from manipulation of equilibrium properties like in light-enhanced superconductivity, to the creation of genuine dynamical states, such as time crystals. To gain insights into the nature of these phenomena, we have extensively studied the effects of external periodic driving in a well-controlled yet versatile many-body platform consisting of ultracold atoms coupled to the light field of a high-finesse optical cavity. In this system, structures in both space and time may emerge due to the rich interplay between driving, dissipation, and long-range atomic interaction mediated by the cavity photons. In this talk, I will discuss the full dynamical phase diagram of the periodically driven atom-cavity system. For off-resonant driving, we observe dynamical control of the self-organisation phase transition. While for resonant driving, we discover the emergence of genuine nonequilibrium phases, namely a dissipative time crystal and dynamical density wave orders. Experimental results confirmed our theoretical predictions of light-induced control in the atom-cavity system.

P02

Boundary time crystals in collective d-level systems

***Luis Fernando dos Prazeres[1], Leonardo da Silva Souza[1], Fernando Iemini[1]**

Instituto de Física[1], Universidade Federal Fluminense, Niterói, Rio de Janeiro, Brasil

arXiv:2102.03374

1. Intrdocution

Boundary time crystals (BTC's) [presented in Ref.[1]] are non-equilibrium phases of matter occurring in quantum systems in contact to an environment, for which a macroscopic fraction of the many body system breaks time translation symmetry. We study BTC's in collective d-level systems, focusing in the cases with $d = 2, 3$ and 4. We find that BTC's appear in different forms for the different cases. In the collective 2-level system we have shown by Jacobian analysis the properties of all steady states of the model illustrated by a complete phase diagram. In a second part of the work we consider a pair of collective interacting 2-level system and it demonstrate to have richer dynamical properties including, limit cycles, period double cascades and chaos. In the third part of the work we consider a pair of collective interacting 2-level system with a shared commom level which presents different dynamical properties from $d = 2$ and $d = 4$.

2. Models

A

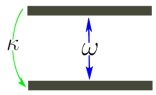

B

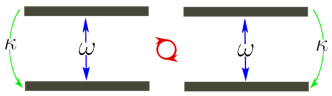

C

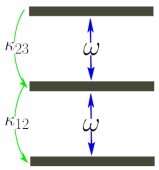

We consider models with collective interactions composed of N d-level subsystems coupled to a Markovian environment. The time evolution for the system is described by the master equation [2],

$$\frac{d}{dt}\hat{\rho} = \hat{\mathcal{L}}[\hat{\rho}] = i[\hat{\rho}, \hat{H}] + \sum_i \left(\hat{L}_i \hat{\rho} \hat{L}_i^\dagger + \frac{1}{2}\{\hat{L}_i^\dagger \hat{L}_i, \hat{\rho}\} \right), \quad (1)$$

A

We start considering the simpler case with $d = 2$. In this case the coherent Hamiltonian and Lindblad jump operators are defined as,

$$\hat{H} = \omega_0 \hat{S}^x + \frac{\omega_x}{S}(\hat{S}^x)^2 + \frac{\omega_z}{S}(\hat{S}^z)^2, \quad (2)$$

$$\hat{L} = \sqrt{\frac{\kappa}{S}}\hat{S}_-, \quad (3)$$

where $S = N/2$ is the total spin of the system, $\hat{S}^\alpha = \sum_j \hat{\sigma}_j^\alpha/2$ with $\alpha = x, y, z$ are collective spin operators, $\hat{\sigma}_j^\alpha$ are the Pauli spin operators for the j'th subsystem.

B

In this case we consider a model describing a pair of collective 2-level (spin $1/2$) systems. Specifically, we define the coherent Hamiltonian and Lindblad jump operators as follows,

$$\hat{H} = \frac{\omega_{zz}}{S}\hat{S}_1^z\hat{S}_2^z + \frac{\omega_{z-}}{S}\hat{S}_1^z\hat{S}_2^- + \sum_{p=1}^{2}\omega_{xp}\hat{S}_p^x + \omega_{zp}\hat{S}_p^z, \quad (4)$$

$$\hat{L}_1 = \sqrt{\frac{\kappa_1}{S}}\hat{S}_{-,1}, \qquad \hat{L}_2 = \sqrt{\frac{\kappa_2}{S}}\hat{S}_{-,2}, \quad (5)$$

where $S = N/2$ is the total spin of each collective system, $\hat{S}_p^\alpha = \sum_j \hat{\sigma}_{j,p}^\alpha/2$ with $p = 1, 2$, $\alpha = x, y, z$ are the collective spin operators for the p'th collective $1/2$-spin system. The operators $\hat{\sigma}_{j,p}^\alpha$ are the usual Pauli spin operators for the j'th spin in the p'th collective system.

C

In this case the model describe cooperative evolution of a collection of three-level subsystems ($d = 3$). The Lindbladian given as follows,

$$\hat{\mathcal{L}} = (1 - \delta)\hat{\mathcal{L}}_{12} + \delta\hat{\mathcal{L}}_{23}, \quad (6)$$

and Lindblad jump operator ($\hat{L}^{(mn)}$) given by,

$$\hat{H}^{(mn)} = \omega_{mn}\hat{S}^x_{mn}, \qquad \hat{L}_{mn} = \sqrt{\frac{\kappa_{mn}}{S}}\,\hat{S}_{-,mn}. \quad (7)$$

where $S = N/2$ and $\hat{S}^\alpha_{mn} = \sum_{j=1}^{N}\hat{\sigma}^\alpha_{j,mn}/2$ with $\alpha = x, y, z$ and $m, n = 1, 2, 3$ label the pairs of (m, n) levels. The operators $\hat{\sigma}^\alpha_{j,mn}$ are the usual Pauli spin operators for the j'th subsystem in the pair of (m, n) levels.

3. $d = 2$

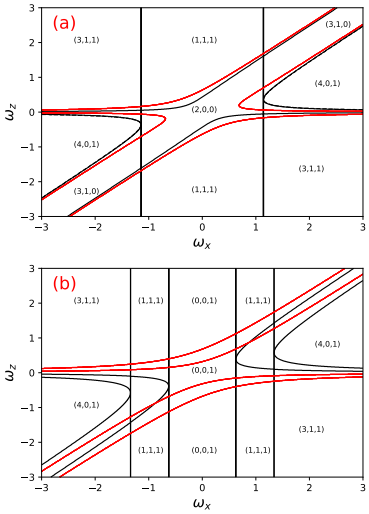

Phase diagram from the collective 2-level system. a) show the weak dissipative, defined as $\frac{\omega}{\kappa} > 1$, phase and b) the strong dissipative phase, defined as $\frac{\omega}{\kappa} < 1$.

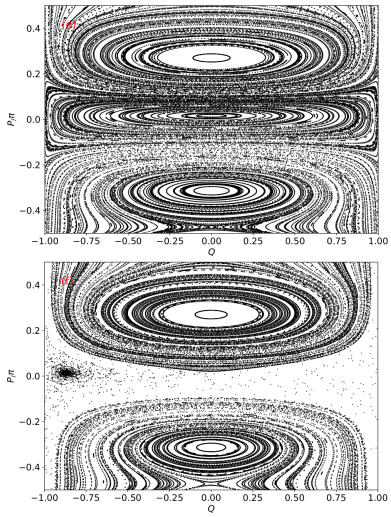

Phase portrait of the observables both in the weak dissipative phase and $\omega_x = 2$, upper panel has $\omega_z = 0$, bottom panel $\omega_z = 3$.

4. $d = 4$

The fixed parameters were

$$\begin{aligned} \omega_{xp} &= 2 \; p = 1, 2, \\ \omega_{z2} &= 0.1, \\ \omega_{xx} &= 3, \\ \omega_{z2} &= 0.02. \end{aligned} \quad (8)$$

The orbit diagram.

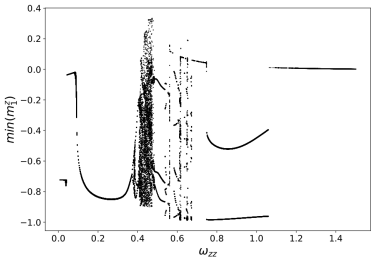

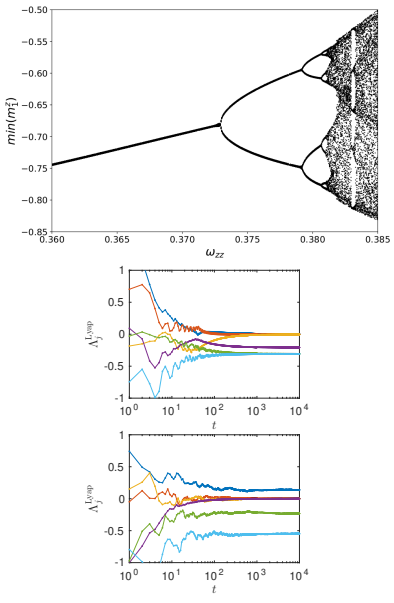

Lyapunov espectrum. Upper panel $\omega_{zz} = 0.35$ and bottom panel $\omega_{zz} = 0.45$

5. $d = 3$

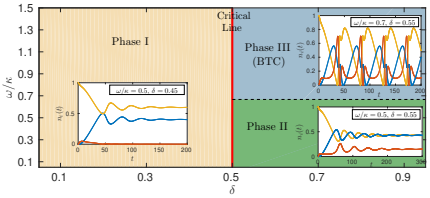

Phase diagram from $d = 3$ level system.

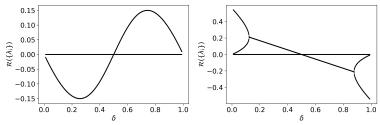

Real parts of the jacobian spectrum from the steadies states of the $d = 3$ level system, showing a change of stability in $\delta = 0.5$.

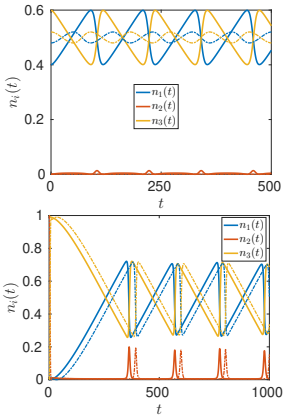

Evolution of the number operators in the critical line $\delta = 0.5$ and $\frac{\omega}{\kappa} = 0.2$.

6. Article

References

[1] F. Iemini, A. Russomanno, J. Keeling, M. Schirò, M. Dalmonte, and R. Fazio. Boundary time crystals. *Phys. Rev. Lett.*, 121:035301, Jul 2018.

[2] M.A. Nielsen and I.L. Chuang. *Quantum Computation and Quantum Information*. Cambridge Series on Information and the Natural Sciences. Cambridge University Press, 2000.

P03

Realization of time-space lattices

Time crystalline structures are characterized by regularity that single-particle or many-body systems manifest in the time domain, closely resembling the spatial regularity of ordinary space crystals. Here we propose a model that, by periodically shaking spatial lattices, the corresponding Wannier states can present crystalline structure in spatial and time domain simultaneously. Our results provide a potential platform to investigate higher order topological phenomena, e.g., six-dimensional quantum Hall effect.

P04

Anderson Molecules

Paweł Matus
Krzysztof Giergiel
Krzysztof Sacha

krzysztof.giergiel+am@gmail.com
Atomic Optics Department
Marian Smoluchowski Institute of Physics
Jagiellonian University in Krakow

Abstract

Atoms can form molecules if they attract each other. This poster shows, that atoms are also able to form bound states not due to the attractive interaction but because of destructive interference. If the interaction potential changes in a disordered way with a change of the distance between two atoms, Anderson localization can lead to the formation of exponentially localized bound states. While disordered interaction potentials do not exist in nature, it is shown that they can be created by means of random modulation in time of the strength of the original interaction potential between atoms and thus objects dubbed Anderson molecules[1,2] can be realized in the laboratory.

Anderson Molecule

$$H = \frac{p_1^2}{2m} + \frac{p_2^2}{2m} + V(r_{12}),$$

Center of mass can be separated. Taking $p_{12} = p_1 - p_2$ we are left with standard Anderson localization Hamiltonian:

$$H = \frac{p_{12}^2}{m^*} + V(r_{12}),$$

$V(r_{12})$ is a random function with infinite support. Free particle in random potential scatters and due to desctructive interference localizes or diffuses anomalously slowly. In localized regime one expect exponential localization in relative distance:

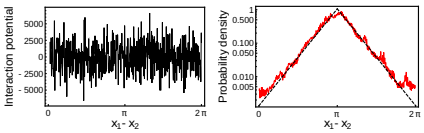

Engineering of time structures

Integrable 1D system: $(z, p) \to (\theta, J)$:

$$H_0(x,p) \longrightarrow H_0(J) \implies J = const, \quad \theta = \frac{\partial H_0(J)}{\partial J} t + \theta_0,$$

Let us add periodic perturbation:

$$H_1 = \lambda \cos(k\omega t)\, V(x) \longrightarrow H_1 = \lambda \cos(\omega t) \sum_n g_n(J) \exp(in\theta).$$

Let's look at the resonant driving:

$$\omega = \frac{\partial H_0(J_r)}{\partial J_r}.$$

The system in the rotating frame:

$$\Theta = \theta - \omega t \text{ , for } J \approx J_r : \dot{\Theta} = \frac{\partial H(J)}{\partial J} - \omega \approx 0,$$

Effective Hamiltonian:

Lowest order H_0: $P = J - J_r \approx 0 \Longrightarrow H_0 \approx \frac{P^2}{2m_{eff}}$,
Averaging over the fast time variable:

$$H_{eff} = \langle H \rangle_t = \frac{\hat{P}^2}{2m_{eff}} + V_0 \cos(k\hat{\Theta}).$$

In the quantum description $J_r^{-1} = -i[x,p]$ is an effective Planck constant. For $J_s \gg 1$ (large ω), the quantization, i.e., when $P \to -i\frac{\partial}{\partial\Theta}$, provides the same results as eigenstates of full quantum description:

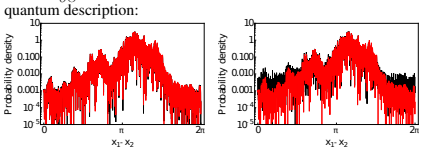

Particles on a ring

Two atoms with the same mass but in different hyperfine states on a ring moving with the angular velocities $\pm\omega$. When interaction stregth between atoms is modulated in time in a disordered way, a diatomic Anderson molecule can form.

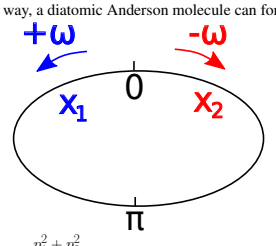

$$H = \frac{p_1^2 + p_2^2}{2} + 2\pi[\lambda_0 + \lambda f(t)]\delta(x_1 - x_2),$$

$\lambda_0 = mR\omega_\perp a_s/(\pi\hbar)$, where a_s - atomic s-wave scattering length $\omega_\perp$ - the frequency of the harmonic transverse trapping potential. Both a_s and $\omega_\perp$ are tunable parameters. Lets drive them:

$$f(t+T) = f(t) = \sum_{k=-k_m}^{k_m} f_k e^{ik\omega t},$$

where $T = 2\pi/\omega$ and $f_{-k} = f_k^*, f_0 = 0$.

For resonant ω rotating frame unitary transformation is $H \to UHU^\dagger + i(\partial_t U)U^\dagger$, with:

$$U(t) = \exp[i\omega t(p_1 - p_2)] \cdot \exp[-i\omega(x_1 - x_2)],$$

and results in

$$H = \frac{p_1^2 + p_2^2}{2} + \sum_{n=-\infty}^{\infty} \left(\lambda_0 + \lambda \sum_{k=-k_m}^{k_m} f_k e^{ik\omega t}\right) e^{in(x_1 - x_2 + 2\omega t)},$$

After time averaging we obtain:

$$H_{rel} = p^2 + \lambda \sum_{n=-k_m/2}^{k_m/2} f_{-2n} e^{inx},$$

$|\psi(x_1, x_2, t)|$ in the moving frame of reference. Initial state is a Gaussian with the variance $\sigma^2 = 0.001$, $\lambda = 2000$ and $k_m = 500$. The localization results are valid if $\omega \gg 10^5$.

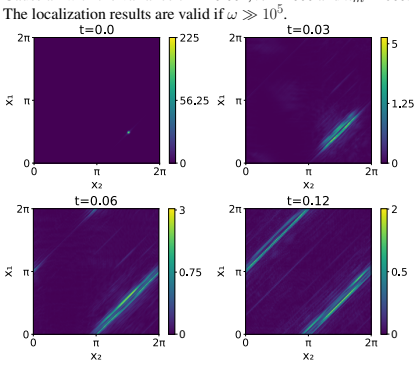

Particles on a line

Two atoms which move initially with the velocity ω on a line

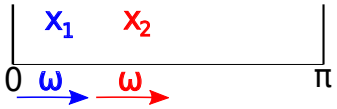

Action - angle coordinates:

$$J_i = |p_i|, \quad x_i = |\theta_i|,$$
$$H = \frac{J_1^2 + J_2^2}{2} + 2\pi\lambda f(t)\,[\delta(\theta_1 - \theta_2) + \delta(\theta_1 + \theta_2)].$$

Moving frame of reference:

$$\Theta_1 = \theta_1 - \omega t, \qquad I_1 = J_1 - \omega,$$
$$\Theta_2 = \theta_2 - \omega t, \qquad I_2 = J_2 - \omega,$$

where $\omega = J_1 = J_2$ is the frequency of the periodic modulation. Following the same procedure with time averaging:

$$H_{\text{eff}} = \frac{I_1^2 + I_2^2}{2} + \lambda \sum_{n=-k_m/2}^{k_m/2} f_{-2n} e^{in(\Theta_1 + \Theta_2)}.$$

The same as Hamiltonian for atoms on a ring!
Anderson molecule in laboratory frame:

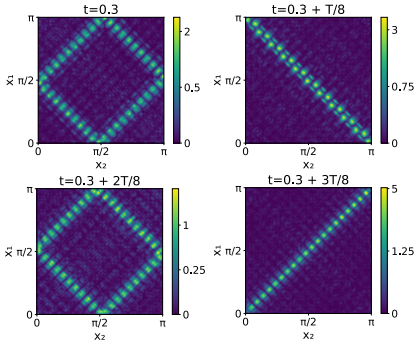

Particles in a box

Two atoms with the same initial velocity in a 3D potential well. In 3D there is localized-delocalized transition. Transition can be observed for fixed disorder by changing the energy of a particle.

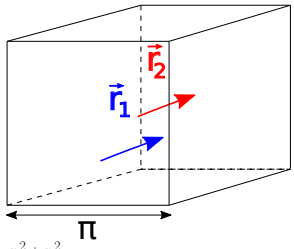

$$H = \frac{\mathbf{p}_1^2 + \mathbf{p}_2^2}{2} + 2(2\pi)^3 [\lambda_0 + \lambda f_1(t) f_2(t) f_3(t)]\, \delta(\mathbf{r}_1 - \mathbf{r}_2),$$
$$f_j(t) = \sum_k f_k^{(j)} e^{ik\omega_j t},$$

with $\lambda_0 = a_s/(4\pi L)$, $f_0^{(j)} = 0$ and $f_k^{(j)} = f_{-k}^{(j)*}$ independent random numbers.
Ratios of ω_1, ω_2 and ω_3 are irrational numbers. Initial velocities components x, y and z are close to the values ω_1, ω_2 and ω_3. Under these conditions effective description on 3D flat torus is given by:

$$H_{\text{eff}} = \frac{\mathbf{I}_1^2 + \mathbf{I}_2^2}{2} + 2\lambda V_1(\Theta_{x_1} + \Theta_{x_2}) V_2(\Theta_{y_1} + \Theta_{y_2}) V_3(\Theta_{z_1} + \Theta_{z_2}),$$

where $V_j(\Theta) = \sum_k f_{-2k}^{(j)} e^{ik\Theta}$. For just relative positions we get:

$$H_{\text{eff}} = \mathbf{P}^2 + 2\left[\frac{\mathbf{P}^2}{2} + V(\mathbf{r})\right],$$
$$V(\mathbf{r}) = \lambda V_1(x) V_2(y) V_3(z).$$

Second order perturbative terms are proportional to $\frac{\lambda^2}{(k\omega_1 + m\omega_2 + n\omega_3)^2}$, hence irrationality condition.

Interacting Anderson molecules

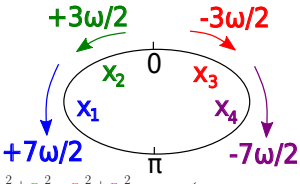

$$H_{\text{eff}} = \frac{{p_1}^2 + {p_2}^2}{2} + \frac{{p_3}^2 + {p_4}^2}{2} + \lambda \sum_n \left(f_{-2n} e^{in(x_1 - x_2)} + e^{in(x_3 - x_4)}\right),$$

Turning on the Fourier harmonics divisible by 3, 5 and 7 we get:

$$H_{\text{eff}} = E_{a,0} + E_{b,0} + \frac{P_a^2 + P_b^2}{4} + V_{ab}(X_a - X_b),$$

with tunable interaction potential $V_{ab}(X_a - X_b)$:

$$\lambda \sum_n \left[f_{-3n} e^{-in(r_a + r_b)} + f_{-5n} 2\cos(n(r_a - r_b)) + f_{-7n} e^{in(r_a + r_b)}\right] \times \frac{e^{in(X_a - X_b)}}{\left(1 + l_a^2 n^2/4\right)\left(1 + l_b^2 n^2/4\right)}.$$

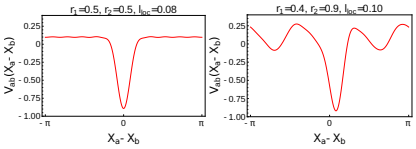

Perspectives

- Understanding spectra of an Anderson molecules.
- Formation of multi atom bound systems.
- Anderson molecule chemistry.

References

[1] K. Giergiel, A. Miroszewski, and K. Sacha, Phys. Rev. Lett. **120**, 140401 (2018)

[2] P. Matus, K. Giergiel, K. Sacha, arXiv:2009.02344, (2021)

Acknowledgments

We are grateful to Peter Hannaford for discussion and valuable comments. Support of the National Science Centre Poland via Projects No. 2016/20/W/ST4/00314 and 2019/32/T/ST2/00413 (K.G.) and 2018/31/B/ST2/00349 (K.S.) is gratefully acknowledged. K.G. acknowledges the support of the Foundation for Polish Science (FNP).

P05

Phase diagram and optimal control for n-tupling discrete time crystal

Arkadiusz Kuroś,[1] Rick Mukherjee,[2] Weronika Golletz,[1,*] Frederic Sauvage,[2] Krzysztof Giergiel,[1] Florian Mintert,[2] and Krzysztof Sacha[1]

[1] *Instytut Fizyki Teoretycznej, Uniwersytet Jagielloński, ulica Profesora Stanisława Łojasiewicza 11, PL-30-348 Kraków, Poland*
[2] *Blackett Laboratory, Imperial College London, SW7 2AZ, UK*

Spontaneous symmetry breaking is a fundamental concept in many areas of physics. The (space) crystals, superconductors and ferromagnets are respective examples of continuous space translation, gauge and rotational invariance breaking. Despite its popularity, the idea of breaking the continuous time translation symmetry and the discrete time-translation symmetry (DTTS) has received attention only very recently and manifested in the form of the *discrete time crystals* [1–4].

It was shown that isolated periodically driven ultracold atoms [2] are able to spontaneously self–reorganise their motion leading to DTTS breaking. Here we focus on these kinds of systems bouncing resonantly on an oscillating atom mirror with the interaction between atoms greater than a critical value. Such a driven cloud of ultracold atoms moves with a period n-times longer than that of the mirror (n:1 resonance condition of motion is fulfilled) due to DTTS breaking, and the so-called n-tupling discrete time crystals (nDTC) is formed.

These systems are promising for experimental realisation [5]. As experimental conditions are never perfect, we analyse the robustness of nDTC against small perturbations of initial state by determining the phase diagrams using Bayesian optimisation. Moreover, we investigate quantum many-body fluctuations of nDTC resulting from interactions between atoms in the Bogoliubov approximation [6].

[1] F. Wilczek, *Phys. Rev. Lett.* 109, 160401 (2012)
[2] K. Sacha, *Phys. Rev. A* 91, 033617 (2015)
[3] V. Khemani *et al.*, *Phys. Rev. Lett.* 116, 250401 (2016)
[4] D. Else *et al.*, *Phys. Rev. Lett* 117, 090402 (2016)
[5] K. Giergiel *et al.*, *New J. Phys.* 22, 085004 (2020)
[6] A. Kuroś *et al.*, *New J. Phys.* 22, 095001 (2020)

* weronika.golletz@doctoral.uj.edu.pl

P06

Stroboscopic aliasing in long-range interacting quantum systems

We unveil a mechanism for generating oscillations with arbitrary multiplets of the period of a given external drive, in long-range interacting quantum many-particle spin systems. These oscillations break discrete time translation symmetry as in time crystals, but they are understood via two intertwined stroboscopic effects similar to the aliasing resulting from video taping a single fast rotating helicopter blade. The first effect is similar to a single blade appearing as multiple blades due to a frame rate that is in resonance with the frequency of the helicopter blades' rotation; the second is akin to the optical appearance of the helicopter blades moving in reverse direction. Analogously to other dynamically stabilized states in interacting quantum many-body systems, this stroboscopic aliasing is robust to detuning and excursions from a chosen set of driving parameters, and it offers a novel route for engineering dynamical n-tuplets in long-range quantum simulators, with potential applications to spin squeezing generation and entangled state preparation.

P07

Dissipative Time Crystals in an atom-cavity system

We are experimentally exploring the light-matter interaction of a Bose-Einstein condensate (BEC) with a single light mode of an ultra-high finesse optical cavity. The key feature of our cavity is the small field decay rate (/2 ≈ 4.5 kHz), which is in the order of the recoil frequency (/2 ≈ 3.56 kHz). This leads to a unique situation where cavity field evolves with the same timescale as the atomic distribution. If the system is pumped with a steady state light field, red detuned with respect to the atomic resonance, the Hepp-Lieb-Dicke phase transition is realized. Starting in this self-ordered density wave phase and modulating the amplitude of the pump field, we observe a dissipative discrete time crystal, whose signature is a robust subharmonic oscillation between two symmetry-broken states [1]. On the other hand, modulation of a phase of the pump field can give rise to an incommensurate time crystal as proposed in [2]. For a blue-detuned pump light with respect to the atomic resonance, we propose an experimental realization of limit cycles. Since the model describing the system is time-independent (DC-driven), the emergence of a limit cycle phase heralds the breaking of continuous time-translation symmetry [3]. By periodically driving, the limit cycles stabilize and the system undergoes a transition from a continuous to a discrete time crystal [4]. [1] H. Keßler et al., arXiv:2012.08885v2 (2021) [2] J. G. Cosme et al., PRA 100, 053615 (2019) [3] H. Keßler et al., PRA 99, 053605 (2019) [4] H. Keßler et al., New J. Phys., 22(8), 085002.

P08

Non-separable time-crystal structures on the Möbius strip

Krzysztof Giergiel[1], **Arkadiusz Kuroś**[1], **Arkadiusz Kosior**[2] **and Krzysztof Sacha**[1]

1. Instytut Fizyki Teoretycznej, Uniwersytet Jagielloński, ulica Profesora Stanisława Łojasiewicza 11, PL-30-348 Kraków, Poland
2. Max-Planck-Institut für Physik Komplexer Systeme, Nöthnitzer Strasse 38, D-01187, Dresden, Germany

Periodically driven many-body quantum systems provide a comfortable platform for modelling crystalline structure in the time dimension which opens a path to realize temporal condensed matter physics and explore novel phenomena. It has been already shown that the time domain can host Anderson localization, Mott insulator phase [1], topological phases [2], dynamical phase transitions [3], quasi-crystals [4] and fractional time crystals [5].

Here, we present a simple implementation of non-separable two-dimensional lattices with a non-trivial topology in the time domain that can be created for a Bose-Einstein condensate bouncing resonantly between two oscillating mirrors. As an example, we consider a three-band Lieb lattice [6] on the Möbius strip with a middle flat band. The dynamics of the flat band is governed solely by interactions, which can be easily tuned by periodic changes of scattering length using Feshbach resonance mechanism. This allows us to engineer exotic long-range interactions [7] and offers a new perspective for studying exotic many-body dynamics.

References

[1] K . Sacha, Sci. Rep. 5, 10787 (2015).
[2] K . Giergiel, A. Dauphin, M. Lewenstein, J. Zakrzewski, and K. Sacha, NJP 21, 052003 (2019).
[3] A . Kosior and K. Sacha, Phys. Rev. A 97, 053621 (2018).
[4] K . Giergiel, A. Kuroś, and K. Sacha, Phys. Rev. B 99, 220303 (2019).
[5] P . Matus and K. Sacha, Phys. Rev. A 99, 033626 (2019).
[6] S . Taie, H. Ozawa, T. Ichinose, T. Nishio, S. Nakajima, and Y. Takahashi, Science Advances 1 (2015).
[7] K . Giergiel, A. Miroszewski, and K. Sacha, Phys. Rev. Lett. 120, 140401 (2018).

P09

Structural, Electronic, Magnetic and Thermodynamic Properties of XCrGe (X = Hf and Zr) Half-Heusler compounds: First Principle Calculations

Structural, electronic, magnetic and thermodynamic properties of XCrGe (X = Hf and Cr) half-Heusler alloys have been studied using first principle Density Functional Theory (DFT) with the state of the art full-potential linearized augmented plane wave (FP- LAPW) method. Both compounds were observed to be ferromagnetic and half-metallic in nature with a small band gap in their spin up (majority) channels. The Slater-Pauling rule was employed to predict the total magnetic moment of 4μB which agree with the values obtained in the calculation. Their mechanical properties show that they are mechanically stable and ductile in nature. The directional dependences of Young's modulus, shear modulus, Poisson's ratio and linear compressibility (in the xy, xz and yz planes) were presented. This theoretical investigation suggests that the two materials have the potential of being used as spintronics devices.

P10

Dynamical Mean-Field Theory for Markovian Open Quantum Many-Body Systems

Open quantum many body systems describe a number of experimental platforms relevant for quantum simulations, ranging from arrays of superconducting circuits, to ultracold atoms in optical lattices in presence of controlled dissipative processes. In this work we extend the nonequilibrium bosonic Dynamical Mean Field Theory (DMFT) to Markovian open quantum systems. As a first application of this technique, we address the steady-state of a driven-dissipative Bose-Hubbard model with two-body losses and single-body incoherent pump. We show that DMFT captures hopping-induced dissipative processes beyond mean-field, which crucially determine the properties of the normal phase, including the redistribution of steady-state populations, the emergence of quantum-Zeno regimes and the phase transition towards a nonequilibrium superfluid phase. We show that this transition occurs as finite-frequency instability, leading to an oscillating-in-time order parameter.

Towards a Time Crystal in a Bouncing Bose-Einstein Condensate

Ali Zaheer[1], Arpana Singh[1], Tien Tran[1], Chamali Gunawardana[1], Krzysztof Giergiel[2], Krzysztof Sacha[2], Andrei Sidorov[1] and Peter Hannaford[1]

[1] *Optical Sciences Centre, Swinburne University of Technology, Melbourne, Australia*

[2] *M. Smoluchowski Institute of Physics, Jagiellonian University, Krakow, Poland*

We report on an experiment to create a discrete time crystal (DTC) based on a Bose-Einstein condensate (BEC) of ultracold atoms bouncing resonantly on a periodically driven atom mirror [1]. The period of the bouncing atoms is chosen to be an integer multiple s of the oscillation period of the mirror and the interatomic interaction is sufficiently strong to break the discrete time-translation symmetry of the bouncing atoms. Such a system can allow dramatic breaking of time-translation symmetry where the time crystal can evolve with a period typically s = 20 - 100 times longer than the driving period T [2]. We present an experimental protocol for realizing big time crystals.

- **Interaction between atoms causes breaking of discrete time-translational symmetry and system to evolve with period s times longer than driving period T.**
- **Time crystal is robust against perturbations (e.g., variations in drop height), and can in principle persist indefinitely without decay (for large N).**

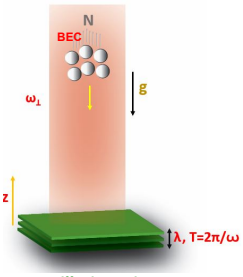

Oscillating mirror

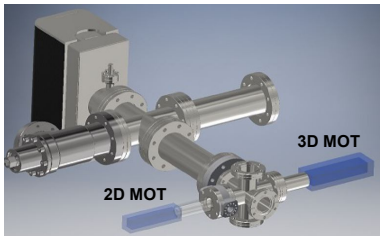

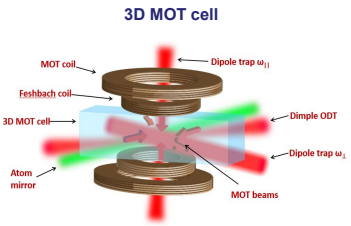

Atomic system

- ^{39}K : 93%, I = 3/2
- D2: 767 nm, D1: 770 nm.
- Broad Feshbach resonance $|1,+1\rangle$ at 403 G, $|\Delta|$=52 G, a_{bg}= -29a_0; allows to tune interaction precisely by varying B (70 times more precise than ^{85}Rb).

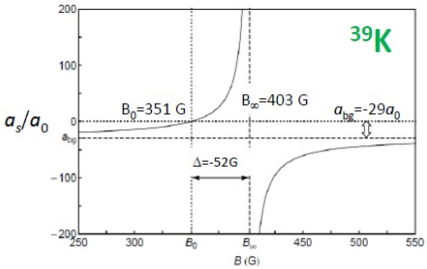

R. Campbell, PhD Thesis, Cambridge

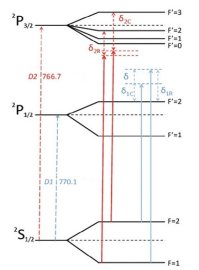

G. Salomon et al., EPL **104**, 63002 (2013)

Mean-field single-particle calculations for s=20-100 [2]

- Calculated parameters for different values of s for ^{39}K atoms for hard-wall mirror with λ=0.2 (gravitational units), bandgap $\Delta E/J$=10, N_{bounce}=54.

s	Mirror freq [kHz]	Mirror ampl [nm]	Drop height [μm]	Tunnel time [s]
20	2.4	8.6	85	0.45
30	2.7	6.5	145	0.59
40	3.1	5.4	213	0.71
60	3.5	4.1	365	0.93
80	3.8	3.4	536	1.13
100	4.1	2.9	722	1.31

Mean-field calculations [2]

Optimized occupation probability of localized wave-packets for s=30

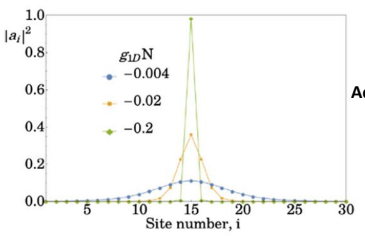

Phase-space map for soft gaussian mirror (s=30 resonance islands near I=1200)

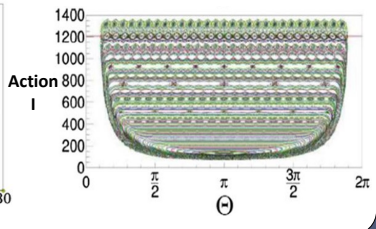

Parameters for realistic soft Gaussian mirror (s=30) [2]

$$V(z) = V_0 \exp\left(-z^2/2\sigma_0^2\right)$$

- Optimal mirror amplitude required to give stable 30:1 resonance islands: $\lambda \approx 75$ nm (for V_0/V_{max}=0.8, σ_0=15.5, V_{max}=4.6x10^3).
- Tune mirror frequency $\omega/2\pi$ = 2.8 kHz for T_{bounce} = 30T, h = 145 μm.

Amplitude of Fourier components

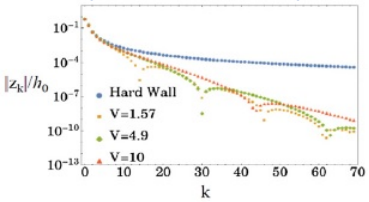

Optimal mirror amplitude

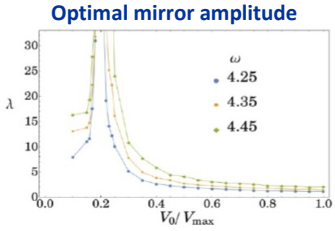

Experimental protocol

1. Prepare ^{39}K BEC

- 2D MOT beam ⇒ 3D MOT; grey molasses with blue-detuned D1 line ⇒ ~5 μK; Crossed optical dipole trap with $\omega_\perp/2\pi=\omega_{||}/2\pi$=95 Hz; evaporatively cool to ~100 nK ⇒ BEC.

2. Release BEC from optical dipole trap

- Prepare BEC (~5000 atoms) at h = 145 μm; set $\omega_{||}$ = 0 to create optical waveguide (1064 nm, 95 Hz); BEC falls on light-sheet mirror (532 nm, 3 W, waist 10 μm, horiz extension 200 μm).

3. Adjust mirror dynamics for s=30

- For s = 30 and h = 145 μm, require mirror frequency $\omega/2\pi$ = 2.8 kHz, and for optimum mirror height (V_o/V_{max} = 0.8), require λ = 75 nm.

4. Detect discrete time crystal

Measure atom density at fixed positions:

(i) $g_{1D}N$ = 0, decays after 54 bounces (due to tunnelling between wave-packets)

(ii) $g_{1D}N$ = -0.2, stable evolution of wave-packet after 54 bounces (t/T = 2200) ⇒ DTC.

Signature of formation of discrete time crystals s=40 [3]; Initial state: harmonic trap
Snapshots after 55 bounces

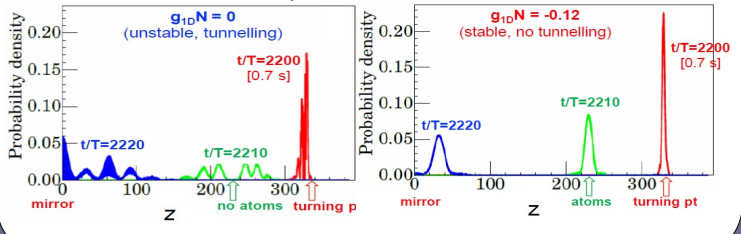

Condensed matter physics in time domain with bouncing BEC [3,4]

- Anderson localization with temporal disorder.
- Many-body localization with temporal disorder.
- Dynamical quantum phase transitions in time domain.
- Time quasi-crystals.
- Many-body systems with exotic, long-range interactions in time domain.
- Topological time crystals.

1. K. Sacha, *Phys. Rev. A* **91**, 033617 (2015)
2. K. Giergiel, T. Tran, A. Zaheer, A. Singh, A. Sidorov, K, Sacha and P. Hannaford, *New J. Phys.* **22**, 085004 (2020)
3. K. Giergiel, A. Kosior, P. Hannaford and K. Sacha, *Phys. Rev. A* **98**, 013613 (2018)
4. P. Hannaford and K. Sacha, *Phys. World* **33**, 42 (2020)

P12

Incommensurate time crystalline dynamics in a atom-cavity system

Periodically driven atoms in a high finesse optical cavity enjoy a very rich phase diagram. By off resonant driving the equilibrium properties of the system can be renormalised in a controlled fashion, while resonant driving allows for new non-equilibrium phases such as time crystalline phases and dynamical density wave orders as recently reported. In this talk, I will discuss the emergence of a incommensurate time crystal by a phase-modulated transverse pump field, resulting in a shaken lattice. This shaken system exhibits macroscopic oscillations in the number of cavity photons and order parameters at noninteger multiples of the driving period, which signals the appearance of an incommensurate time crystal. The subharmonic oscillatory motion corresponds to dynamical switching between symmetry-broken states, which are nonequilibrium bond ordered density wave states. Employing a semiclassical phase-space representation for the driven-dissipative quantum dynamics, we confirm the rigidity and persistence of the time crystalline phase. We identify experimentally relevant parameter regimes for which the time crystal phase is long lived, and map out the dynamical phase diagram. I will further present preliminary experimental results that confirm our theoretical predictions.

P13

On the long-term stability of space-time crystals

We investigate a space-time crystal in a superfluid Bose gas. Using a well-controlled periodic drive we excite only one crystalline mode in the system, which can be accurately modeled in the rotating frame of the drive. Using holographic imaging we observe the stability of the crystal over an extended period of time and show the robustness of its structure in both space and time. By introducing a fourth-order term in the Hamiltonian we show that the crystal stabilizes at a fixed number of quanta. The results of the model are compared to the experimental data and show good agreement, with a small number of free parameters. The results yield insights in the long-term stability of the crystal, which can only be obtained by the combination of the extended control in the experiment and the nearly ab initio character of the model. From the model we derive a phase diagram of the system, which can be exploited in the future to study the phase transitions for this new state of matter in even more detail.

P14

Many-body localization with synthetic gauge fields in disordered Hubbard chains

The phenomenon of many-body localization (MBL) is attracting significant theoretical and experimental interest over the past few years. The signatures of MBL have been observed in recent cold-atom experiments in optical lattices. The recent experimental advances of synthetic gauge fields allow us to explore the MBL with magnetic flux. We discuss the role of synthetic magnetic fields on the localization properties of disordered fermions. The spectral statistics exhibit a transition from ergodic to MBL phase, and the transition shifts to larger disorder strengths with increasing magnetic flux. The dynamical properties indicate the charge excitation remains localized whereas spin degree of freedom delocalized in the presence of synthetic flux. The full localization of spin excitation can be recovered when spin-dependent disorder potential is realized. Furthermore, we show the effect of quantum statistics on the local correlations and show that the long-time spin oscillations of a hard-core boson system are destroyed in contrast to the fermionic case.

P15

Universal Aspects of Vortex Reconnections across the BCS-BEC Crossover

Reconnecting vortices in a superfluid allow for the energy transfer between different length scales and its subsequent dissipation. Present picture assumes that the dynamics of a reconnection is driven mostly by the phase of the order parameter, and this statement can be justified in the case of Bose- Einstein Condensates (BECs), where vortices have simple internal structure. Not much has been said about this relation in the context of Fermi superfluids. We aim at bridging this gap, and we report our findings, which reveal that the reconnection dynamics conforms with the predicted universal behaviour across the entire BCS-BEC crossover. The universal scaling survives also for spin-imbalanced systems, where unpaired fermions induce a complex structure of the colliding vortices.